Optimal Integration of Distributed Generators (DGs) Shunt Capacitors (SCs) and Electric Vehicles (EVs) in a Distribution System (DS) using Marine Predator Algorithm

Nagaraju Dharavat*, Suresh Kumar Sudabattula**‡, Velamuri Suresh**

* School of Electronics and Electrical Engineering, Lovely Professional University, Phagwara, Punjab, India, 144411

** Symbiosis Institute of Technology, Symbiosis International (Deemed University), Pune, India, 412115

(nagaraju.dnr98@gmail.com, suresh.21628@lpu.co.in, velamuri.suresh@gmail.com)

‡ Corresponding author, e-mail: suresh.21628@lpu.co.in

Received: 05.07.2022 Accepted: 01.09.2022

Abstract- In this paper, a combined approach based on voltage stability index (VSI) and Marine predators algorithm (MPA) is proposed to solve the problem of distributed generators (DGs), Shunt Capacitors (SCs) and Electric Vehicles (EVs) allocation in the distribution system (DS). Further, the objective of this method is to minimize power loss (P^{Loss}) and enhance the voltage profile of the DS. Also, the developed method is tested on practical 83 bus Taiwan DS. The static and dynamic load variations are considered to study the performance. EV charging and discharging patterns are considered to check the performance of DS. Different cases such as single DG, multiple DGs, and the combination of DGs plus SCs, DGs plus EVs are considered to check the method's effectiveness. Finally, the results related to grid vehicle (G2V), vehicle to grid (V2G), conventional charging and optimized charging are projected. The suggested MPA with DA, GOA and WOA methods are thoroughly compared under various DS operating circumstances. The obtained results verified that proper placement of DGs and effective charging strategies for EVs reduce the P^{Loss} to a considerable extent.

Keywords: Distributed Generations (DGs), Electric Vehicles (EVs), Marine Predators Algorithm (MPA), Power Loss, Voltage profile, Shunt Capacitors (SCs)

1. Introduction

In recent years the utilization of electrical power increased drastically. In another way, the power generation through conventional power plants decreased because of the non-availability of the fuel resources. Also, the usage of electric vehicles (EVs) throughout the globe is increasing positively. This creates a further burden on the distribution system (DS). To address this problem, it is vital to use distributed energy resources (DERs) optimally. Installing locally distributed generators (DGs) close to the customer and adding shunt capacitors (SCs) to the system can increase network capacity, save operational costs, minimise losses, and enhance voltage profile and stability [1]. Power engineers use SCs for reactive power adjustment in DS. DGs mostly depend on renewable generation resources (RER) such as sunlight (Solar), air (Wind), geothermal systems, and biofuels. Still, it also considers energy sources like combustion engines, combined heat and power (CHP) and diesel engines on a limited scale. But, it is vital to place DGs in optimal locations to shrink power loss (P^{Loss}) and ameliorate voltage profile. Incorrect placement of DG causes more P^{Loss} and voltage drop [2].

The demand to integrate DGs, SCs and EVs in radial DS has grown in recent years due to their scientific, commercial, ecological, and economical aspects, including increased power grid efficiency, reduced P^{Loss}, and improved voltage profile,. However, if the integration of DGs, SCs, and EVs is not planned improperly, tech problems arise, such as overvoltage, instability, and system imbalance [3]. Further, the total demand throughout the globe increased drastically. Also, EV charging and discharging patterns further degrade DS performance. It is vital to incorporate

DGs, SCs and EVs considering proper charging and load patterns to solve the above-mentioned issue[4].

Table 1. Different techniques summary of with and without optimal placement of DGs, SCs and EVs in DS

Reference	Objective	Optimisation Method	Test System	Year
DGs To DS				
[6]	Reducing active power loss, cost and GHG emission, increasing reliability and voltage	TLBO	17-bus	2018
[7]	Minimizing P^{Loss}, increasing VSI	CNF	IEEE 30 bus	2018
[8]	Decreasing power loss and fuel cost	ABC, GSA	IEEE 9 bus	2019
[9]	Power loss reduction, VSI maximization	ASFLA	IEEE 33 & 69-bus	2019
[10]	Shrinking power loss and energy losses. Revamping voltage profile	SS-CFLCP	25-city grid in Tennessee	2020
[11]	Revamping voltage stability and resilience, minimising voltage deviation and power loss	PFA	IEEE 33, 69 bus	2021
[12]	Decreasing power loss, improving Voltage stability and voltage profile	CMPSO	33-bus, 274-bus	2022
SCs To DS				
[13]	Decreasing energy losses and enhancing voltage profile	GA, EA, PSO	IEEE 123 feeder	2018
[14]	Reducing real P^{Loss} and annual energy losses Agumenting voltage profile and stability	GA	IEEE 33	2019
[15]	Reducing P^{Loss} & voltage fluctuation, increasing voltage stability and profile	PSO	IEEE 33 and Brazil-136 Bus	2020
[16]	Decreasing P^{Loss} & enhancing voltage profile	MSFLA	95 & 136-buses	2021
[17]	Alleviated P^{Loss} & Augmenting voltage profile	SHARD, SOE	33 & 59-buses	2022
EVs TO DS				
[18]	Reducing loss and operational cost	TOPSIS, GWO	38-bus	2018
[19]	Active power loss reduction	GWOA, GA	69-bus	2019
[20]	Minimizing P^{Loss} & voltage deviation	GA	IEEE 33-bus	2020
[21]	Decreasing power loss	PLM method	IEEE 33	2021
[22]	Reducing cost	SOC Based CCM	RBTS 2-Bus	2021
[23]	Improving voltage profile, energy	BVBSOA	IEEE 69, IEEE 119-bus	2022
DGs + SCs To DS				
[24]	Voltage and load fluctuation, minimizing power loss	GA-PSO	IEEE 33	2018
[25]	Improving reliability and voltage profile	HOM	IEEE 33, IEEE 69	2019
[26]	Reducing daily power loss	PSO-OPF, IPM	Bus 2,3, 4, 5, 6,7, 9, 10	2020
[27]	Reducing power loss, enhancing voltage stability and voltage stability	EGOA	IEEE 33	2021
[28]	The increasing ability of the system, decreasing power loss, maintenance cost	RO, KDE	IEEE 33, 25-bus	2022

The authors solved the placement of DG problem and investigated numerous test systems. In majority published papers, decreasing the P^{Loss} alone is the only objective function studied. The authors contemplated integrating reactive power generating sources into the DS[6-12]. Few researchers have investigated the simultaneous integration of DGs and SCs into DS. Compared to their single distribution, the combination of DGs and SCs proved more efficacious [13-17]. The increased operating performance of the DS in the existence of EVs is not the prime motive of the operations being discussed. In [18-23] authors solved the impact of EVs on the DS studied.

In the literature, authors solved DGs, SC and EVs integration problems in DS to minimize P^{Loss} and enhance the voltage profile. Further, [24-28] authors solved DGs and EVs problem by considering EV charging stations and other charging-related issues, organising best charging and discharging schedules when distributing energy supplies, etc. But, simultaneous allocation of DGs,

SCs and EVs with considering charging and discharging patterns of EVs needs more attention and provides more positive results. In this paper, the authors solved DG and EV allocation problems using a combined voltage stability index (VSI) approach and marine predator algorithm (MPA). Further, the developed method's effectiveness is studied on practical 83 bus Taiwan DS. Different case studies are considered to check the efficacy of the proposed approach.

The content of the article is organised as follows: The mathematical problem formulation objective and its constraints are discussed in section 2. Integrated solutions for optimal installation and sizing of DGs, SCs and EVs in section 3. In section 4, Results & Discussions are discussed. EV charging and discharging patterns are explained in section 5. Finally, the conclusion of the article is given in section 6.

2. Mathematical Problem Formulation:

The primary objective is to minimise the P^{Loss} of the DS and the total voltage deviation of all buses with the optimal integration of DGs, SCs and EVs. The active, reactive P^{Loss} and voltage injection at specific bus equations are given below

$$P_{k+1} = P_k - P_{Lk+1} - R_{k,k+1}.\frac{P_k^2+Q_k^2}{|V_k|^2} \quad (1)$$

$$Q_{k+1} = Q_k - Q_{Lk+1} - X_{k,k+1}.\frac{P_k^2+Q_k^2}{|V_k|^2} \quad (2)$$

$$|V_{k+1}|^2 = |V_k|^2 - 2\left(R_{k,k+1}.P_k + X_{k,k+1}.Q_k\right) + (R_{k,k+1}^2 + X_{k,k+1}^2).\frac{P_k^2+Q_k^2}{|V_k|^2} \quad (3)$$

Where at node k → P_k= Real power, Q_k= Reactive power

At node k+1 → P_{Lk+1}= Real power load, Q_{Lk+1}= Reactive power load

The line section between nodes k and k+1 → $R_{k,k+1}$= Resistance, $X_{k,k+1}$= Reactance

k^{th} node voltage magnitude = $|V_k|$

equation (1) & (2) represents power balance

Eq's (3) fulfils sending and receiving end of voltage magnitude

Eq 4 reprsents active P^{Loss}

$$min \sum_{k=1}^{24} P^{Loss}(k) \quad (4)$$

Where

$$P^{Loss}(k) = \sum_{k=1}^{24} I^2.R_k \quad (5)$$

Adding all line losses = total P^{Loss} represented by below eq

$$Total\ P^{Loss} = \sum_{k=0}^{n-1} P^{Loss}\ (k.k+1) \quad (6)$$

$$P_{DGSC}^{Loss(k,k+1)} = R_{k,k+1}.\left(\frac{P_{DGSC,k,k+1}^2 + Q_{DGSC,k,k+1}^2}{|V_k|^2}\right) \quad (7)$$

$$P_{DGSC}^{TotalLoss(k,k+1)} = \sum_{k=1}^{nbk} P_{DGSC}^{Loss(k,k+1)} \quad (8)$$

$$y_1 = \Delta P_{DGSC}^{TotalLoss} = \frac{P_{DGSC}^{TotalLoss}}{P^{TotalLoss}} \quad \text{or} \quad y_1 = minimize(P^{Loss}) \quad (9)$$

$$y_2 = maximize(VSI) = minimize\left(\frac{1}{VSI}\right) \quad (10)$$

$$Objective\ Function = y_1 \times w_1 \times y_2 \times w_2 \quad (11)$$

2.1 Constraints

Power balance Constraints

$$\sum_{k=1}^{24} P_G(k) = \sum_{k=1}^{24} P_D(k) + P_{SC}(k) + P^{Loss}(k) \pm P_{EV}(k) \quad (12)$$

Voltage Constraints

$$V_{k,min} \le |V_k| \le V_{k,max} \quad (13)$$

DG Size Constraints

$$P_{k,min}^{DG} \le P_k^{DG} \le P_{k,max}^{DG} \quad (14)$$

Where,

$$\left(P_{k,min}^{DG} = 0.1 \sum_{k=2}^{n} P_m^{DG}, P_{k,max}^{DG} = 0.8 \sum_{k=2}^{n} P_k^{DG}\right)$$

SC Size Constraints:

$$\sum_{k=1}^{nc} Q_{cl} \le 1.0 \sum_{k=1}^{n} Q_c^L \quad (15)$$

$Q_{cl} = JQ_0 \quad J = 1, 2 \ldots..n_c$

Q_0 = minimum SC size, J = integer number

Different constraints integrated with EVs are

EVs Battery storage Constraints:

EVs k^{th} hour state of charge is

$$SoC_{min,k} \le SoC_k^{EV} \le SoC_{max,k} \quad (16)$$

Charging /Discharging EV Constraints:

EV power charging/discharging must be within below equation limits

$$P_{ch,k} \le P_{ch,k}^{max} \quad (17)$$

$$P_{disch,k} \le P_{disch,k}^{max} \quad (18)$$

Where, $P_{ch,k}$, $P_{disch,k}$ = EV battery k^{th} hour charging & discharging power

3. Integrated Solutions for Optimal Installation and Sizing of DGs, SCs and EVs

3.1 Different types of EVs Charging methods:

EV owners will charge their vehicles as soon as they arrive home. In this paper, this strategy is referred to as the conventional charging method (CCM). Demand is used to prioritise EV charging and discharging. This procedure is known as the optimal charging method (OCM). EV consumers are concerned about system load in the OCM method. EV charging is not permitted at peak demand. The scheduling approach considers the

peak-to-average ratio (PAR) of the workload demand. The primary goal of EV scheduling is to reduce the PAR, which is expressed as follows.

$$PAR = \frac{P_{d,peak}}{P_{d,mean}} \quad (19)$$

Where $P_{d,mean}$ = average system demand, $P_{d,peak}$ = peak system demand

The charging or discharging is determined by the power ratio (PR), which is indicated as follows. Here are two important points must follow, EVs are permitted to charge if the PAR is less than 1; else, it will check again in an hour. The number of EVs allocated must not be negative.

$$P_R = \frac{P_D(n)}{P_{d,mean}} \quad (20)$$

$$\sum_{t=1}^{N} EV_{pit} \leq EV_T \quad (21)$$

3.2 Finding a Suitable Location with VSI to Place DGs, SCs and EVs in DS:

[5]developed VSI first, following VSI identified the optimal installation of DGs, SCs and EVs in DS. All buses are assessed based on the analytical VSI value, and a bus is considered strong if the VSI value is near one. Any bus is considered weak if the predicted value is near zero (0). This approach selects the stronger buses for EV deployment, while the weaken buses are considered for renewable DGs and SCs allocation. This way, the best location for deploying renewable DGs, SCs and EVs is to examine.

$$VSI = |V_k|^4 - 4\left[P_{k+1.eff}X_k - Q_{k+1.eff}R_k\right]^2 - 4\left[P_{k+1.eff}R_k + Q_{k+1.eff}X_k\right]|V_k|^2 \quad (22)$$

3.3 Marine Predators Algorithm (MPA):

MPA is a meta-heuristic optimisation technique known as the natural behaviour of marine predators. It follows an ideal strategy between prey and predator. Predators can use an adaptive encounters ratio policy, and prey can use this approach to implement an optimal foraging strategy. In MPA, the prey-to-predator speed ratio is critical. Levy's flight is used to represent prey and predator movement. In various behaviours, marine predators take advantage of their excellent spatial memory and cognitive abilities., including food retrieval and memorising sites where they frequently locate food [29-30].

$$X_0 = X_{min} + rand(X_{max} - X_{min}) \quad (23)$$

X_{min} = Lower variable, X_{max}= Upper Variable, rand is a uniformly distributed random vector with a value ranging from 0 to 1.

$$Elite = \begin{bmatrix} X_{1,1}^I & X_{1,2}^I & \dots & X_{1,d}^I \\ X_{2,1}^I & X_{2,2}^I & \dots & X_{2,d}^I \\ \vdots & \vdots & \dots & \vdots \\ \vdots & \vdots & \dots & \vdots \\ X_{n,1}^I & X_{n,2}^I & \dots & X_{n,d}^I \end{bmatrix} \quad (24)$$

$$Prey = \begin{bmatrix} X_{1,1} & X_{1,2} & \dots & X_{1,d} \\ X_{2,1} & X_{2,2} & \dots & X_{2,d} \\ \vdots & \vdots & \dots & \vdots \\ \vdots & \vdots & \dots & \vdots \\ X_{n,1} & X_{n,2} & \dots & X_{n,d} \end{bmatrix} \quad (25)$$

$\vec{X}^I$= Predator top vector, n= No.of times Elite matrix, d = No. of dimensions

MPA Initialization Process:

The MPA procedure comprises three significant steps dependent on the flow rate, which are shown below

Phase 1 ($V \geq 10$):

When there is a large flow rate, the predator is going quicker than the prey. This circumstance occurs during the earliest optimisation stages when exploration is essential.

While $Iter < \frac{1}{3}Max\_Iter$

$\overrightarrow{Stepsize_\iota} = \overrightarrow{R_B} \otimes (\overrightarrow{Elite_\iota} - \overrightarrow{R_B} \otimes \overrightarrow{Prey_\iota})$
i = 1,…...n

$\overrightarrow{Prey_\iota} = \overrightarrow{Prey_\iota} + P.\vec{R} \otimes \overrightarrow{Stepsize_\iota}$ (26)

Where, Iter = Current Iteration, Max_Iter = Maximum No.of Iterations, $\otimes$ = Multiplication

P = 0.5, $\vec{R}$ = 0 to 1Ranges, $\overrightarrow{R_B}$ = Brownian motion-based normal distributed vector

Phase 2($V = 1$):

The predator and prey travel at the same speed, which is known as a unit velocity ratio. It's as though they're both on the hunt for their prey. This segment happens during the optimisation process' intermediate phase when the exploration is attempting to be transiently changed to exploitation [29-30].

While $\frac{1}{3}\ Max\_Iter < Iter < \frac{2}{3}\ Max\_Iter$

1st half population

$\overrightarrow{Stepsize_\iota} = \overrightarrow{R_L} \otimes (\overrightarrow{Elite_\iota} - \overrightarrow{R_L} \otimes \overrightarrow{Prey_\iota})$ i = 1,….n/2

$\overrightarrow{Prey_\iota} = \overrightarrow{Prey_\iota} + P.\vec{R} \otimes \overrightarrow{Stepsize_\iota}$ (27)

Where, $\overrightarrow{R_L}$ = random vector, it depends mainly on Levy distribution

2nd half population

$\overrightarrow{Stepsize_\iota} = \overrightarrow{R_B} \otimes (\overrightarrow{R_B} \otimes \overrightarrow{Elite_\iota} - \overrightarrow{Prey_\iota})$
i = n/2,….,n

$$\overrightarrow{Prey_i} = \overrightarrow{Elite_i} + P.CF \otimes \overrightarrow{Stepsize_i} \quad (28)$$

While $CF = (1 - \frac{Iter}{Max\_Iter})^{(2\frac{Iter}{Max\_Iter})}$

Where CF = adaptive parameter, it controls the predator step size

$\overrightarrow{R_B} \otimes \overrightarrow{Elite_i}$ = Brownian behaviour of predator move

Phase 3 ($V = 0.1$):

When there is a low-velocity ratio, the predator goes quicker than the prey. This situation occurs near the optimisation process's end, typically attributed to high exploitation capacity.

While $Iter > \frac{2}{3}Max\_Iter$

$\overrightarrow{Stepsize_i} = \overrightarrow{R_L} \otimes (\overrightarrow{R_L} \otimes \overrightarrow{Elite_i} - \overrightarrow{Prey_i})$ i = 1,….n

$$\overrightarrow{Prey_i} = \overrightarrow{Elite_i} + P.CF \otimes \overrightarrow{Stepsize_i} \quad (29)$$

FAD Impact and Eddy Formation:

Environmental factors such as eddy formation or the impact of Fish Aggregating Devices (FADs) also influence behavioural changes in marine predators [26].

$$\overrightarrow{Prey_i} = \begin{cases} \overrightarrow{Prey_i} + CF[\vec{X}_{min} + \vec{R} \otimes (\vec{X}_{max} - \vec{X}_{min})] \otimes \vec{U} & if\ r \le FADs \\ \overrightarrow{Prey} + [FAD(1-r) + r](\overrightarrow{Prey}_{r1} - \overrightarrow{Prey}_{r2}) & if\ r > FADs \end{cases} \quad (30)$$

FAD = 0.2, $\vec{U}$ =Binary vector [0, 1], r = random vector [0,1], r_1, r_2 = prey matrix

$\vec{X}_{max}$, $\vec{X}_{min}$ = dimensions of upper and lower bounds, Fig (1) represent MPA pseudocode.

Initialize Prey populations i=1,...,n
While finish criteria is not met
Calculate the fitness and construct the Elite matrix
If Iter < Max_Iter/3
Update prey based on (26)
Else if Max_Iter/3<Iter<2*Max_Iter/3
For the first half of the populations (i=1,...,n/2)
Update prey based on (27)
For the other half of the populations (i=n/2,...,n)
Update prey based on (28)
Else if Iter >2*Max_Iter/3
Update prey based on (29)
End (if)
Accomplish memory saving and Elite update
Applying FADs effect and update based on (30)
End While

Fig. 1. Pseudo code MPA [29]

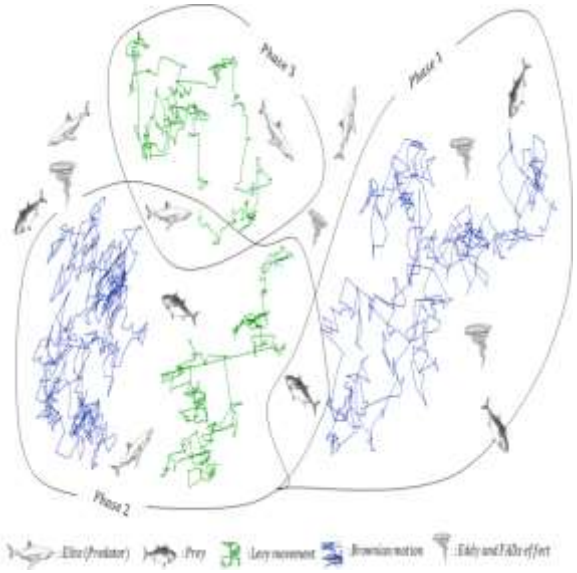

Fig. 2. All the MPA optimisation phases [29]

3.4 Steps for calculating optimal sizes of DGs, and SCs with MPA

Step 1: Read the DS data (Line and Bus data)

Step 2: Run the base-case load flow

Step3: calculated DGs, SCs and EVs locations by VSI tech

Step 4: suitable sites of DGs, SCs, & EVs found with VSI must be given as input to MPA

Step 5: Optimize MPA and Initialize search agents (prey) for i=1,….n

Step 6: determined the fitness value

Step 7: constructed the elite & prey matrices

Step 8: Phase 1 ($V \ge 10$): While $Iter < \frac{1}{3}Max\_Iter$

Step 9: update prey position based on eq. 26

Step 10: Phase 2($V = 1$): While $\frac{1}{3}\ Max\_Iter < Iter < \frac{2}{3}\ Max\_Iter$

Step 11: Prey based on the first half of the population updated with eq. 27

Step 12: Prey updates depending on population 2nd half eq.28

Step 13: Prey position is updated depending on eq. 29

Step 14: Apply FADs effect and update status using eq.30

Step 15: This is the final step, evaluate the objective function of P^{Loss} and places such as suitable DGs and SCs sizes.

4. Results and Discussion:

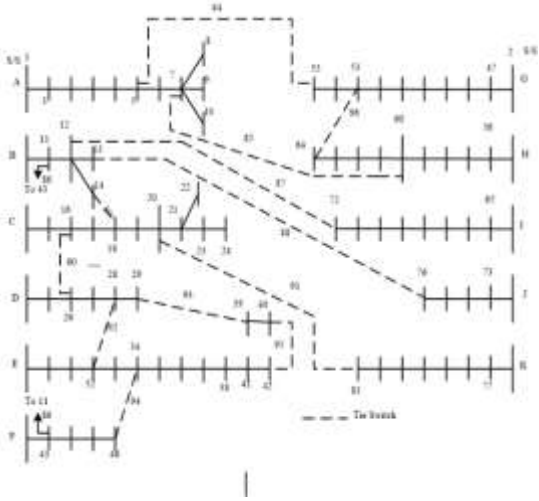

Fig. 3. Practical 83 Taiwan test system [31]

In this work, analyzed different case studies to optimize DGs, SCs and EVs in DS. The simulation was performed on a practical 83 Taiwan real test system. Fig.3 represents the 83 test system. The system configurations are as follows: Voltage:11.4 kV, real and reactive power demands are 28.35 MW & 20.70 MVAr [1], bus data and line data taken from this [31]. The impact of the simultaneous allocation of DGs and SCs in DS and the effect of EV charging on DS are analyzed with different operating conditions. The combination of VSI and MPA is presented to minimize P^{Loss} and augment voltage profile, and the stability of DS is discussed in detail in this section. The load demand curve for analysis is given in Fig.4.

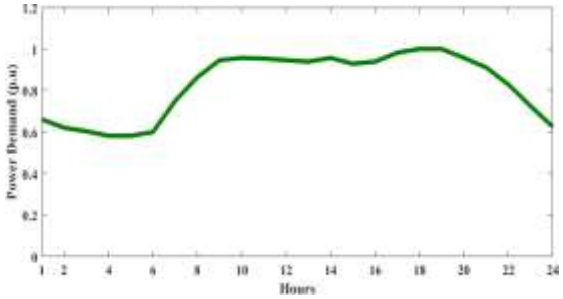

Fig. 4. Power demand curve variation for a typical day

Base Case (Without Considering DGs and SCs):

In this case, without considering DGs & SCs, base case P^{Loss} = 531.9945kW, V_{min} = 0.9277 p.u, VS_{Imin} = 0.7086 p.u. The same mentioned in table 2.

Case 1: With a Single DG Allocation:

With the VSI method identified, 6 is the suitable location to place a single DG. The same information was passed to MPA and found DG size was 2.7903MW, P^{Loss} = 453.1625kW, V_{min} = 0.9472 p.u, VSI_{min}= 0.7533 p.u. With the compared base case, 14.8181% of P^{Loss} was reduced.

Case 2: With Considering Single DG + Single SC:

As per VSI, 6, 8 buses are the best location to insert single DG + single SC. The same message is given to the MPA method; it determines the ranges of DGs and SCs in DS. The MPA size of DGs and SCs is 3.1464MW, and 2.2124MVAr, respectively. P^{Loss} = 406.1333 kW, V_{min} = 0.9472 p.u VSI_{min}= 0.7533 p.u compared to the base case and case 1, case 2 performs better in all aspects.

Case 3: With Two DGs, Without SCs:

Multiple DGs without SCs considered in this case and found that 6 and 79 are the locations to insert 2 DGs as per VSI analysis. According to MPA, DG1 and DG 2 sizes are 3.0579 MW and 3.6439 MW. P^{Loss} = 404.5866kW, V_{min} = 0.9482 p.u, VSI_{min}= 0.7533 p.u.

Case 4: With Considering Two DGs + Two SCs:

Following VSI, 6 and 79 are the best sitting to allocate muti DGs and SCs in DS. The message given to MPA finds the capacity of the muti DGs and DS. DG1, DG2, SC1 and SC2 capacities are 3.0425MW, 3.622 MW, 2.2079 MVAr, and 2.6161 MVAr, respectively. Compared to the above cases with 2 DGs + 2 SCs, 35.7708% of P^{Loss} decreased.

Case 5: With Three DGs Allocation, Without SCs:

According to the VSI method, 6, 71, and 79 are the optimal sites to include 3 DGs. The information sent to the MPA identifies the size of the 3 DGs. The data is contained in table 2. P^{Loss} = 366.422kW, V_{min} = 0.9558 p.u, VSI_{min}= 0.8266 p.u.

Case 6: With Considering Three DGs + Three SCs:

As per the VSI method, 6, 71, and 79 are suitable sites to place three DGs + three SCs. The details are given to MPA, which finds the size of DGs and SCs. Compared to the above cases of three DGs + three SCs, 47.1702% of P^{Loss}.

Case 7: With Four DGs Allocation, Without SCs:

By the VSI, 6, 71, 79, and 83 is the best location for four DGs. The info is transferred to MPA and which determines the capacities of four DGs given in table 2. Further, P^{Loss} decremented, V_{min}, VSI_{min} revamped compared to other cases.

Case8: Considering Four DGs + Four SCs:

The optimal locations of the multi (Four DGs + Four SCs) were found with the VSI technique. By the VSI, 6, 33, 71, and 79 are suitable areas for multi DGs and SCs. The same message was

forward to MPA, identifying ranges of multi DGs and SCs. P^{Loss} minimized, V_{min}, VSI_{min} augmented in this case compared to other cases.

Case 9: Without SCs, with Five DGs Allocations:

P^{Loss} reduced, V_{min}, VSI_{min} increased compared to other cases. According to the VSI technique, 6, 19, 34, 71, and 79 are the apt locations to install five DGs. The same was communicated to MPA, which finds the size of five DGs tabulated in table 2.

Case 10: With Considering five DGs + five SCs:

The VSI method finds the best sites to allocate five DGs + five SCs, as per VSI 6, 19, 34, 71, and 79 for multi DGs and SCs. The same message was communicated to MPA, examining the size of five DGs + five SCs tabulated in table 2.

Table 2. Optimal allocation of DGs and SCs using MPA

Different Cases	DG Size(MW)	SC Size(MVAr)	P^{Loss} (kW)	V_{min} (p.u)	VSI_{min} (p.u)	% of Reduced P^{Loss}
Base Case	NA	NA	531.9945	0.9277	0.7086	NA
Case 1	2.7903 (6)	NA	453.1625	0.9472	0.7533	14.8181
Case 2	3.1464 (6)	2.2124 (8)	406.1333	0.9472	0.7533	23.6583
Case 3	3.0579 (6) 3.6439 (79)	NA	404.5866	0.9482	0.7553	23.9491
Case 4	3.0425 (6) 3.622 (79)	2.2079 (6) 2.6161 (79)	341.6957	0.9482	0.7553	35.7708
Case 5	3.0578 (6) 2.5676 (71) 3.6471(79)	NA	366.422	0.9558	0.8266	31.1229
Case 6	3.1135 (6) 2.5515 (71) 3.6213 (79)	2.2542 (6) 1.9781 (71) 2.6157 (79)	281.0511	0.9599	0.8266	47.1702
Case 7	3.0577 (6) 2.5672 (71) 2.4119 (79) 1.2209 (83)	NA	361.2495	0.9558	0.8266	32.0952
Case 8	3.1473 (6) 3.3721 (33) 2.700 (71) 3.8861 (79)	2.2173 (6) 3.087 (33) 2.648 (71) 3.6404 (79)	233.649	0.9648	0.8266	56.0805
Case 9	3.1946 (6) 3.5429 (33) 2.6628 (71) 3.732 (78) 0.4835 (82)	NA	331.8868	0.9549	0.825	37.6146
Case 10	3.6835 (6) 4.9683 (19) 3.5254 (34) 2.3659 (71) 4.2641 (79)	2.3986 (6) 4.1882 (19) 3.8613 (34) 3.5757 (71) 3.2037 (79)	225.1575	0.9663	0.8266	57.6767
Case 11	2.2586 (6) 3.1933 (19) 2.952 (34) 2.6092 (53) 2.5677 (71) 3.0167 (81)	NA	269.3452	0.9556	0.8272	49.3706
Case 12	3.3549 (6) 4.7731 (19) 4.4148 (34) 2.5497 (53) 2.9541 (71) 4.4177 (81)	2.3667 (6) 2.3857 (19) 3.6122 (34) 3.0371 (53) 2.1475 (71) 3.3041(81)	161.9149	0.9673	0.8317	69.5645

Case 11: Considering Six DGs Without SCs:

The optimal placement of six DG locations is identified with the VSI method. By VSI, 6, 19, 34, 53, 71, and 81 are suitable to place six DGs. The same message was sent to MPA, which determines the size of six DGs. Compared to the above cases, 49.3706% of P^{Loss} was minimized. Voltage profile and voltage stability enhanced. It injects only real (kW) into the system. Fig. 7 represents MPA converges significantly less time to compared other meta-heuristic methods. Table 2 shows the P^{Loss}, V_{min}, and VSI_{min} of six DGs.

Case 12: With Considering Six DGs + six SCs:

Following VSI, 6, 19, 34, 53, 71, and 81 are the best site to place six DGs + Six SCs it injects both the active (kW) and reactive power (kVAr) into the DS. The same information is given to the MPA and found in the six DGs and six SCs sizes included in table 2. Fig. 8 shows the convergence characteristics of the practical 83 test system, proving that, compared to other optimization methods DA, GOA and WOA, MPA performance is outstanding in all aspects.. 69.5645% of P^{Loss} was minimized, higher than all other cases. Fig. 5 and 6 show that Compared to the base case results, decreased P^{Loss}, voltage profile, and voltage stability augmented with MPA. From all 12 cases, the multi (DGs + SCs) efficiency system overall performance improved.

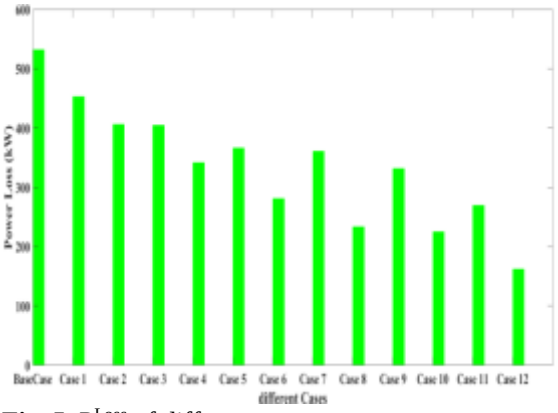

Fig. 5. P^{Loss} of different cases

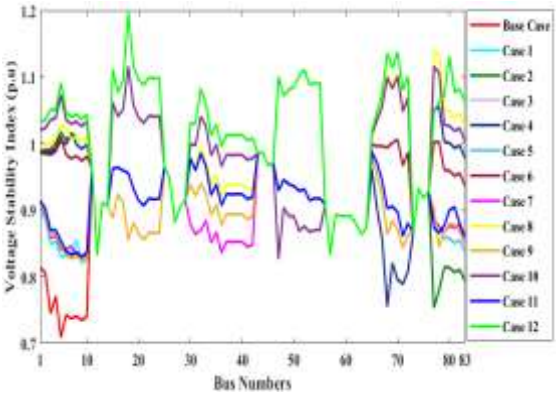

Fig. 6. VSI of 83 bus systems with different cases

4.1 Optimal Capacity of DGs at Different Load Levels Without Considering SCs and EVs:

First, the developed approach is tested for 1 DG, 2 DGs, 3 DGs, 4 DGs, 5 DGs, and 6 DGs combined with SCs 6 DGs + 6 SCs. Table 2 shows the results. The results show that 6DGs and 6 DGs +6 SCs reduce P^{Loss}, enhance voltage profile, and increase VSI. Due to network size and load, the proposed DS can only have 6 DGs + 6 SCs. beyond 6 DGs, system performance will decrease. Now, the proposed approach is tested with half (0.5 per unit), full (1.0 p.u.), and heavy (1.1 p.u.) loads. DGs at all load levels in proper locations and sizes reduce P^{Loss} and enhance voltage profile. Table 3 shows various loads' P^{Loss}, voltage profile, and VSI.

In addition, the suggested MPA is compared in terms of several metrics to other current optimisation methods such as the DA, WOA and GOA. Table 4 shows the results of simulations of all optimisation approaches across 50 trials and 100 maximum iterations. It can be demonstrated that MPA achieves more significant P^{Loss} reduction than any other method. Further, the convergence curve is shown in Fig 7 and 8.

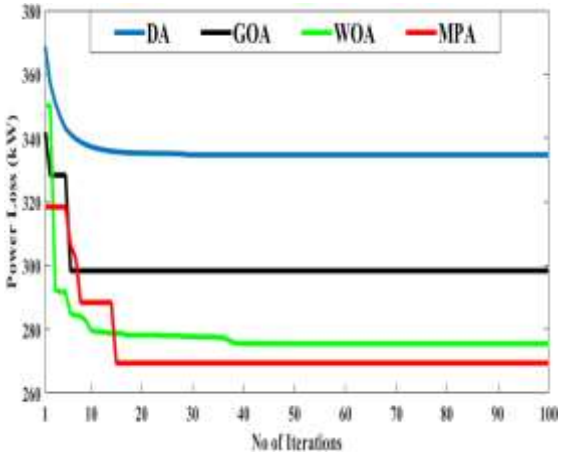

Fig.7. Convergence curve with 6DGs

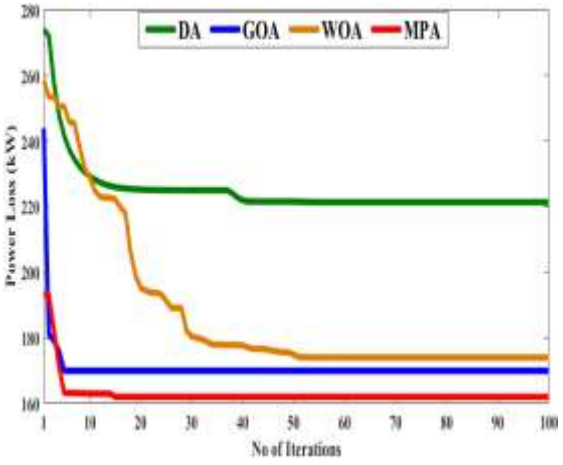

Fig.8. Convergence curve (6DGs+6SCs.

Table 3. Simulation result with different load conditions

Different Loads	DG Sizes (MW)	Base Case P^{Loss} (kW)	With DGs P^{Loss} (kW)	V_{min} (p.u)	VSI_{min} (p.u)
Half Load (0.5)	1.6837 2.5745 2.2930 1.8619 1.6452 1.5368	127.2119	73.2732	0.9787	0.9141
Full Load (1.0)	3.1766 3.5680 2.9319 2.8107 2.5979 2.9823	531.9945	269.3452	0.9556	0.8272
Heavy Load (1.1)	3.4897 3.8800 3.3705 2.9318 2.8519 3.3299	649.8343	330.2084	0.95	0.8075

Table 4. Comparison of MPA with other algorithms

Optimisation methods		P^{Loss} (kW)	Vmin (p.u)	VSImin (p.u)	% of reduced P^{Loss}
Base Case		531.9945	0.9277	0.7086	NA
6 DGs	DA	334.6975	0.9457	0.7553	37.0862
	GOA	298.3518	0.9486	0.8192	43.9182
	WOA	275.4243	0.9501	0.8216	48.2279
	MPA	**269.3452**	**0.9556**	**0.8272**	**49.3706**
6 DGs+ 6SCs	DA	221.359	0.9482	0.7553	58.3907
	GOA	169.915	0.9492	0.8194	68.0607
	WOA	173.9416	0.9537	0.8219	67.3038
	MPA	**161.9149**	**0.9673**	**0.8317**	**69.5645**

4.2 Dynamic performance analysis of practical 83 Taiwan real test system with 6 DGs:

Because the load fluctuates from hour to hour, it's critical to examine the system's dynamic changes. Figure 4 depicts a typical 24-hour load curve. Using the combined technique of VSI and MPA, the analysis described in 12 cases is expanded for a typical 24-hour simulation in this section. The load flow is simulated with dynamic changes in system demand, and the VSI approach is used to decide the best placements of DGs and SCs for all hours. In general, DGs and SCs will be immovable resources in any system. As a result, the determined place should be unique for all dynamic changes in system demand. The optimal sites for all dynamic load changes have been determined as 6, 19, 34, 53, 71, and 81. Table 5 shows the ideal DG sizes for the dynamic instances, whereas Table 6 shows the P^{Loss}, V_{min}, and VSI_{min} determined using MPA. V_{min} and VSI_{min} are clearly within permitted limits for the whole 24-hour period. Fig.9 shows P^{Loss} reduction, and Fig.10 and 11 show voltage profile and stability improvement compared to the base case.

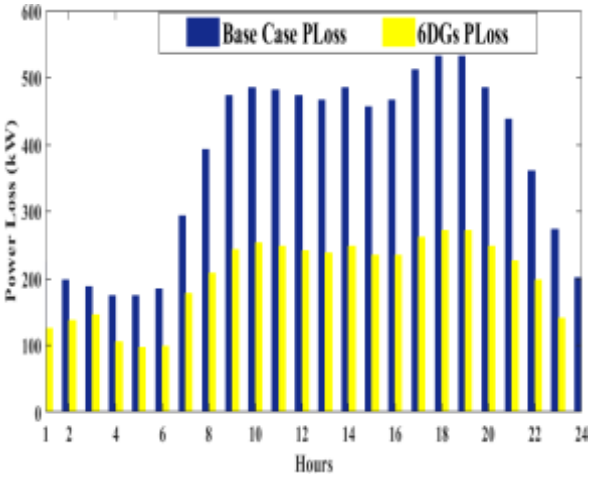

Fig. 9. Dyanmic P^{Loss} Comparison with Base Case

Table 5. dynamic variation of 6 DG Sizes

Hours	DG_1 (MW)	DG_2 (MW)	DG_3(MW)	DG_4 (MW)	DG_5 (MW)	DG_6 (MW)
1	2.0971	2.6283	2.6304	2.4971	1.8764	2.8702
2	1.5986	4.9334	2.9550	2.4631	1.9483	2.1902
3	2.1323	4.6577	2.6879	2.4961	2.2704	3.7751
4	2.0930	3.8788	1.8828	2.3519	1.7717	1.9207
5	1.7763	3.2622	2.2078	1.6188	1.5590	1.8294
6	1.9164	2.6300	2.3162	1.9284	1.8267	1.8357
7	2.8500	2.9453	2.9710	3.5507	3.2213	2.9069
8	2.6382	3.9740	3.3265	2.3749	2.2623	2.5102
9	3.0158	3.1554	2.9096	2.4288	2.4785	2.8862
10	3.1169	3.8757	3.1326	3.0866	2.8540	2.6798
11	2.9809	3.1537	3.3801	2.7205	2.4552	3.1765
12	3.0021	3.0194	2.7914	2.4673	2.4277	2.7966
13	2.9726	2.9842	2.8270	2.4755	2.4229	2.7680
14	3.0371	3.0554	2.8245	2.4967	2.4566	2.8291
15	2.9830	3.4627	2.8300	2.5103	2.3330	2.7547
16	3.0401	3.5820	2.6878	2.6987	2.3330	2.7419
17	3.1174	3.1348	2.8985	2.5620	2.5207	2.9034
18	3.1754	3.1936	2.9520	2.6096	2.5677	2.9565
19	3.1745	3.2566	2.9728	2.6239	2.5935	2.9639
20	3.0368	3.0553	2.8246	2.4961	2.4566	2.8287
21	2.8738	3.6794	3.1969	2.2638	2.3659	2.8840
22	2.6598	4.1867	3.2481	2.7569	2.2413	2.9688
23	2.3019	2.3358	2.1559	1.9022	1.8581	2.1389
24	2.2056	1.9197	2.6934	2.1339	1.8854	2.4075

Table 6. P^{Loss}, V_{min}, and VSI_{min} for dynamic load variations

Hours	Base Case P^{Loss} (kW)	6-DGs P^{Loss} (kW)	V_{min} (p.u)	VSI_{min} (p.u)
1	225.4259	125.1067	0.9706	0.8833
2	198.2772	137.6305	0.9697	0.8801
3	187.2944	145.6995	0.9748	0.8978
4	173.5694	105.6399	0.976	0.9015
5	173.5694	96.4475	0.9737	0.8951
6	184.758	98.9951	0.9735	0.8943
7	292.5018	177.0059	0.9699	0.8734
8	392.1795	207.6245	0.9604	0.8453
9	473.7037	242.055	0.9574	0.8341
10	485.2784	252.5902	0.9574	0.8339
11	482.1065	248.2071	0.9566	0.8312
12	473.7037	241.8868	0.9573	0.8338
13	466.4172	238.2345	0.9576	0.8347
14	485.2784	247.7133	0.9568	0.8319
15	456.1146	233.8518	0.9584	0.8376
16	466.4172	234.5738	0.9588	0.8391
17	512.153	261.2289	0.9556	0.8276
18	531.9945	271.1965	0.9548	0.8245
19	531.9945	271.2152	0.9548	0.8245
20	485.2784	247.7133	0.9568	0.832
21	437.8848	226.8318	0.9589	0.8394
22	359.9057	196.7103	0.963	0.8548
23	272.7216	140.1724	0.9677	0.8721
24	200.9094	109.6494	0.9739	0.8943

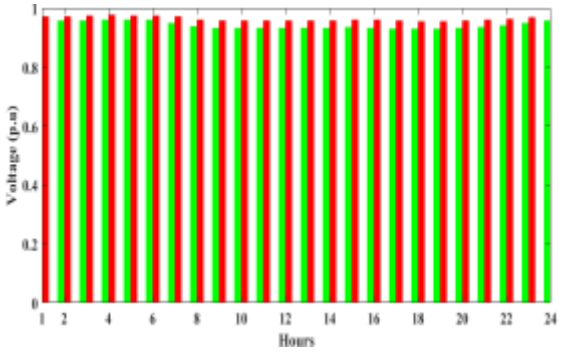

Fig.10. Voltage profile comparison for 24hrs

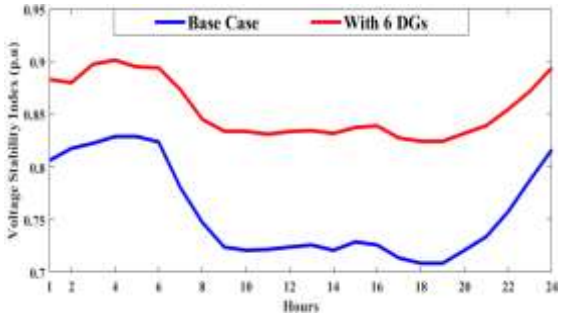

Fig. 11. VSI for 24hrs

5. EV charging Different approaches:

Due to dynamic load variations and rising EV adoption, network conditions weaken. Schedule EVs depend on loading circumstances. This article examines a very well-market-available vehicle Chevy volt EVs. Table 7 lists EV's specifications.

- 60 office-going EVs leave at 8:00 a.m. & arrive at 5:00 p.m.
- All EVs must continue their journey with a fully charged battery and cannot be recharged mid-trip. Depending on the distance travelled/supplied to the system, EV charging takes a significant period of time.
- The technology will offer two-way connectivity between EVs and the system power grid. This inference enables integrated EV and DG scheduling. Thus, data is transferred quickly between channels.

5.1 Conventional Charging Method (CCM):

As per VSI 5, 42, and 78, buses are the best places to charge EVs. The EVs are recharged immediately after receiving their planned journey without concern for network load demand in this technique. The P^{Loss} is calculated every hour, and the results are displayed in Table 8 for 24 hours. During the 18th, 19th, and 20th hours, the EVs are recharged in G2V mode. The voltage profile is affected during the 18-20 hour period due to the increased demand on the network, which affects the system's P^{Loss}. Compared to base case 24hrs P^{Loss} Only EV condition P^{Loss} = 8959.4372kW increased with EVs + DGs P^{Loss} = 4750.2916kW. compared to the base case and only condition, DGs + EVs case 46.9207% P^{Loss} decreased.

5.2 Optimized charging method (OCM):

The EVs will be recharged at off-peak hours defined by the OCM technique. The OCM technique, when combined with MPA-based DGs placement, produces better outcomes than the CCM. Table 8 compares P^{Loss} without EVs and EVs + DGs. Compared to base case 24hrs P^{Loss} Only EV condition P^{Loss} = 8955.131kW increased with EVs + DGs P^{Loss} = 4745.489kW. compared to the base case and only EV, DGs + EVs 46.9744% P^{Loss} decreased. This method reduces more P^{Loss} than CCM.

5.3 Grid to Vehicle + Vehicle to Grid (G 2 V + V 2 G) Method:

Using this technique (G2V Plus V2G), EVs may recharge and transmit electricity back to the grid. The sophisticated method determines when it is optimum to charge the EVs by considering system demand. The EVs will supply electricity to the grid interface between the 18th & 19th hrs in V2G mode. After that, during the 4th and 5th hours, EVs are recharged in G2V mode. Compared to the base case (24 hrs), CCM and OCM approaches, the G 2 V + V 2 G method decreases P^{Loss} more, the same information tabulated in table 8 and shown in Fig.12.

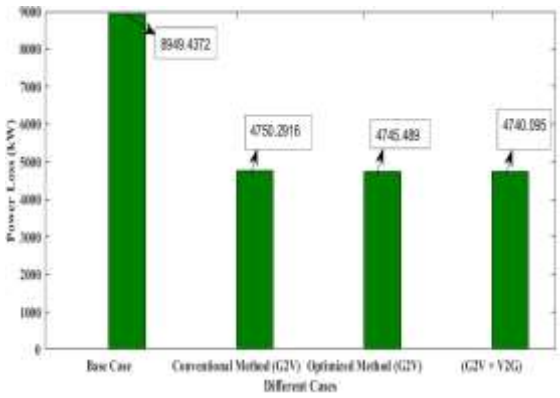

Fig.12. Different EV Charging methods P^{Loss} Comparision with Base Case

Table 7. Specification of EVs

Specification of EVs	**Ranges**
Battery of EV	16 kWh
No. of EVs	60
SoC_{min}	0.2
SoC_{max}	0.9
The average distance each EV travelled	30km

Average electricity use per km	0.175kWh/km

Table 8. Comparisons of different EV Charging methods P^{Loss} for dynamic load variations

Different Cases		**P^{Loss} (kW)**
Base Case		8949.4372
Conventional Method	Only EVs	8959.461
	With EVs + DGs (G 2 V)	4750.2916
Optimized Method	Only EVs	8955.131
	With EVs + DGs (G 2 V)	4745.489
G2V + V2G Method		4740.095

6. Conclusion:

This paper proposes an integrated approach (VSI and MPA) to solve the allocation of DGs, SCs and combined DGs and SCs problems in DS. Further, different load levels are considered, solving the objective function P^{Loss}. Dynamic load variation was considered, determining the sizes of these sources and calculating the objective function. To test the efficacy of the proposed system, 83 bus practical Taiwan DS is considered. Further, various cases are considered, such as single DGs, multiple DGs and SCs, and the obtained results are represented. From the results, the exact placement of multiple DGs and multiple SCs reduces the P^{Loss} from 531.99 k W (base case) to 161.91 kW (6 DGs and 6 SCs), with a good improvement of voltage profile and VSI. The performance of the MPA algorithm is tested and compared with GOA, DA and WOA algorithms. Compared to other algorithms, the MPA algorithm reduces the P^{Loss} to the maximum extent.

Furthermore, office-going EVs are considered and added to the DS and verified the performance. Two charging methods, such as conventional and optimized charging approaches, are taken into account and determine the objective function. Compared to the CCM and the OCM approaches, G2V plus V2G method performed well. This effective charging method reduces the losses and improves the voltage profile and VSI. Finally, an optimal combination of DGs and EVs in the DS improves the overall performance of better loss reduction and enhanced voltage profile and VSI of the system.

Acknowledgements

The authors express their gratitude to the Editor in Chief and Reviewers for the suggestions which enhanced the quality of the paper.

References:

[1] P. P. Biswas, R. Mallipeddi, P. N. Suganthan, and G. A. J. Amaratunga, "A multiobjective approach for optimal placement and sizing of distributed generators and capacitors in distribution network," *Appl. Soft Comput. J.*, vol. 60, pp. 268–280, 2017.

[2] S. R. Gampa and D. Das, "Simultaneous optimal allocation and sizing of distributed generations and shunt capacitors in distribution networks using fuzzy GA methodology," *J. Electr. Syst. Inf. Technol.*, vol. 6, no. 1, pp. 1–18, 2019.

[3] A. Ramadan, M. Ebeed, S. Kamel, E. M. Ahmed, and M. Tostado-véliz, "Optimal allocation of renewable DGs using artificial hummingbird algorithm under uncertainty conditions," *Ain Shams Eng. J.*, no. xxxx, p. 101872, 2022.

[4] V. Suresh, S. Sudabattula, and S. H. C. Cherukuri, "Coordinated power loss minimization technique for Distribution systems in the presence of Electric Vehicles," *2019 Natl. Power Electron. Conf. NPEC 2019*, pp. 1–5, 2019.

[5] R. Ranjan, B. Venkatesh, and D. Das, "Voltage stability analysis of radial distribution networks," *Electr. Power Components Syst.*, vol. 31, no. 5, pp. 501–511, 2003.

[6] M. Khalid, U. Akram, and S. Shafiq, "Optimal planning of multiple distributed generating units and storage in active distribution networks," *IEEE Access*, vol. 6, pp. 55234–55244, 2018.

[7] M. Saleh, Y. Esa, N. Onuorah, and A. A. Mohamed, "Optimal microgrids placement in electric distribution systems using complex network framework," *6th Int. Conf. Renew. Energy Res. Appl. ICRERA 2017*, vol. 2017-Janua, pp. 1036–1040, 2018.

[8] S. Ermis, A. A. Bee, and C. Algorithm, "Optimal Power Flow Using Artificial Bee Colony, Wind Driven Optimization and Gravitational Search Algorithms," *8th Int. Conf. Renew. Energy Res. Appl.*, pp. 963–967, 2019.

[9] A. Onlam, D. Yodphet, R. Chatthaworn, C. Surawanitkun, A. Siritaratiwat, and P. Khunkitti, "Power loss minimization and voltage stability improvement in electrical distribution system via network reconfiguration and distributed generation placement using novel adaptive shuffled frogs leaping algorithm," *Energies*, vol. 12,

no. 3, pp. 1–12, 2019.

[10] R. Kizito, X. Li, K. Sun, and S. Li, "Optimal distributed generator placement in utility-based microgrids during a large-scale grid disturbance," *IEEE Access*, vol. 8, pp. 21333–21344, 2020.

[11] V. Janamala, "A new meta-heuristic pathfinder algorithm for solving optimal allocation of solar photovoltaic system in multi-lateral distribution system for improving resilience," *SN Appl. Sci.*, vol. 3, no. 1, 2021.

[12] G. Derakhshan, H. Shahsavari, and A. Safari, "Co-evolutionary multi-swarm pso based optimal placement of miscellaneous dgs in a real electricity grids regarding uncertainties," *J. Oper. Autom. Power Eng.*, vol. 10, no. 1, pp. 71–79, 2022.

[13] M. Aryanezhad, "Management and coordination of LTC, SVR, shunt capacitor and energy storage with high PV penetration in power distribution system for voltage regulation and power loss minimization," *Int. J. Electr. Power Energy Syst.*, vol. 100, no. February, pp. 178–192, 2018, doi: 10.1016/j.ijepes.2018.02.015.

[14] S. Das, D. Das, and A. Patra, "Operation of distribution network with optimal placement and sizing of dispatchable DGs and shunt capacitors," *Renew. Sustain. Energy Rev.*, vol. 113, no. June, p. 109219, 2019.

[15] K. Balu and V. Mukherjee, "Siting and Sizing of Distributed Generation and Shunt Capacitor Banks in Radial Distribution System Using Constriction Factor Particle Swarm Optimization," *Electr. Power Components Syst.*, vol. 48, no. 6–7, pp. 697–710, 2020.

[16] H. Lotfi, "Optimal sizing of distributed generation units and shunt capacitors in the distribution system considering uncertainty resources by the modified evolutionary algorithm," *J. Ambient Intell. Humaniz. Comput.*, 2021.

[17] M. M. Sayed, M. Y. Mahdy, S. H. E. Abdel Aleem, H. K. M. Youssef, and T. A. Boghdady, "Simultaneous Distribution Network Reconfiguration and Optimal Allocation of Renewable-Based Distributed Generators and Shunt Capacitors under Uncertain Conditions," *Energies*, vol. 15, no. 6, 2022.

[18] J. Singh and R. Tiwari, "Multiobjective Optimal Scheduling of Electric Vehicles in Distribution System," *2018 20th Natl. Power Syst. Conf. NPSC 2018*, pp. 1–6, 2018.

[19] J. Singh and R. Tiwari, "Real power loss minimisation of smart grid with electric vehicles using distribution feeder reconfiguration," *IET Gener. Transm. Distrib.*, vol. 13, no. 18, pp. 4249–4261, 2019.

[20] Z. Huang, B. Fang, and J. Deng, "Multiobjective optimization strategy for distribution network considering V2G-enabled electric vehicles in building integrated energy system," *Prot. Control Mod. Power Syst.*, vol. 5, no. 1, 2020.

[21] A. Sadhukhan, M. S. Ahmad, and S. Sivasubramani, "Optimal Allocation of EV Charging Stations in a Radial Distribution Network Using Probabilistic Load Modeling," *IEEE Trans. Intell. Transp. Syst.*, vol. PP, pp. 1–10, 2021.

[22] [1] M. Akil, E. Dokur, and R. Bayindir, "Impact of electric vehicle charging profiles in data-driven framework on distribution network," *9th Int. Conf. Smart Grid, icSmartGrid 2021*, pp. 220–225, 2021.

[23] M. H. Hemmatpour, M. H. Rezaeian Koochi, P. Dehghanian, and P. Dehghanian, "Voltage and energy control in distribution systems in the presence of flexible loads considering coordinated charging of electric vehicles," *Energy*, vol. 239, p. 121880, 2022.

[24] J. peng Liu, T. xi Zhang, J. Zhu, and T. nan Ma, "Allocation optimization of electric vehicle charging station (EVCS) considering with charging satisfaction and distributed renewables integration," *Energy*, vol. 164, pp. 560–574, 2018.

[25] A. M. Hariri, M. A. Hejazi, and H. Hashemi-Dezaki, "Reliability optimization of smart grid based on optimal allocation of protective devices, distributed energy resources, and electric vehicle/plug-in hybrid electric vehicle charging stations," *J. Power Sources*, vol. 436, no. June, p. 226824, 2019.

[26] K. Gupta, R. Achathuparambil Narayanankutty, K. Sundaramoorthy, and A. Sankar, "Optimal location identification

for aggregated charging of electric vehicles in solar photovoltaic powered microgrids with reduced distribution losses," *Energy Sources, Part A Recover. Util. Environ. Eff.*, vol. 00, no. 00, pp. 1–16, 2020.

[27] S. Velamuri, S. H. C. Cherukuri, S. K. Sudabattula, N. Prabaharan, and E. Hossain, "Combined Approach for Power Loss Minimization in Distribution Networks in the Presence of Gridable Electric Vehicles and Dispersed Generation," *IEEE Syst. J.*, vol. PP, pp. 1–12, 2021.

[28] C. Li, L. Zhang, Z. Ou, Q. Wang, D. Zhou, and J. Ma, "Robust model of electric vehicle charging station location considering renewable energy and storage equipment," *Energy*, vol. 238, p. 121713, 2022.

[29] A. Faramarzi, M. Heidarinejad, S. Mirjalili, and A. H. Gandomi, "Marine Predators Algorithm: A nature-inspired metaheuristic," *Expert Syst. Appl.*, vol. 152, no. March, 2020.

[30] A. S. A. Bayoumi, R. A. El-Sehiemy, and A. Abaza, "Effective PV Parameter Estimation Algorithm Based on Marine Predators Optimizer Considering Normal and Low Radiation Operating Conditions," *Arab. J. Sci. Eng.*, vol. 47, no. 3, pp. 3089–3104, 2022.

[31] J. Chiou, C. Chang, C. Su, and S. Member, "Variable Scaling Hybrid Differential Evolution for Solving Network Reconfiguration of Distribution Systems," *IEEE Trans. Power Syst.*, vol. 20, no. 2, pp. 668–674, 2005.